journal of prosthodontic research 64 (2020) 224–230

Journal of Prosthodontic Research

Original article

Accuracy of removable partial denture framework fabricated by casting with a 3D printed pattern and selective laser sintering

Akinori Tasaka[a,c,*], Takahiro Shimizu[a], Yoshimitsu Kato[a], Haruna Okano[a], Yuki Ida[a], Shizuo Higuchi[b], Shuichiro Yamashita[a]

[a] Department of Removable Partial Prosthodontics, Tokyo Dental College, Tokyo, Japan
[b] Wada Precision Dental Laboratories Corporation, Osaka, Japan
[c] Oral Health Science Center, Tokyo Dental College, Tokyo, Japan

ARTICLE INFO

Article history:
Received 12 May 2019
Received in revised form 18 June 2019
Accepted 22 July 2019
Available online 26 August 2019

Keywords:
Removable partial denture
Metal framework
CAD/CAM
3D-printed pattern casting
Selective laser sintering

ABSTRACT

Purpose: The present study aimed to compare the accuracy of removable partial denture (RPD) frameworks fabricated by 3D-printed pattern casting and those fabricated by selective laser sintering (SLS).

Methods: A partially edentulous mandibular model was used for the simulation model. Scanning of the model was performed using a dental scanner. The framework was designed by using CAD software. The 3D-printed resin pattern was formed using a 3D printer and casting was performed (AM-Cast framework), and a direct metal laser sintering machine was used for the framework of SLS (SLS framework). 3D scanning of fabricated two types of framework were performed, and these data were overlapped with design data. Fabrication accuracy was verified using the Mann–Whitney U test to compare the discrepancy between the AM-Cast and SLS frameworks.

Results: The range of differences for the AM-Cast and SLS framework were -0.185 ± 0.138 to 0.352 ± 0.143 mm and -0.166 ± 0.009 to 0.123 ± 0.009 mm, respectively. Statistically significant differences were observed at the rests, proximal plates, connectors, and clasp arms. Regarding the rests, both lateral and medial displacement in the two types framework was observed in relation to the design data. Large lateral discrepancies of the connectors were observed at the joining area on the tooth-supported side of the lingual bar for the AM-Cast framework. Localized discrepancies were observed at the center of the lingual bar for the SLS framework.

Conclusion: The accuracies of RPD frameworks fabricated by AM-Cast and SLS differ depending on the specific structural component of the RPD.

1. Introduction

The use of computer-aided design and computer-aided manufacturing (CAD/CAM) technology is becoming increasingly widespread in the fabrication of metal frameworks for removable partial dentures (RPD) [1]. With this technology, the framework can be designed on a three-dimensional (3D) model obtained from 3D scans of the working cast [2–5]. The steps of determining the direction of insertion and removal, marking the framework design, block out the working cast, applying relief, and completing the wax-up of the framework that were previously performed using a dental surveyor can now be carried out digitally. By eliminating the need for duplicate impressions and refractory casts required in conventional casting, this digitalization simplifies the fabrication process, reduces material costs, and saves time. The reproducibility of the fabrication process is also increased while differences in fabrication results among dental technicians are minimized [6].

There are currently two predominant methods of applying CAD data to the fabrication of frameworks in clinical settings [7]. One method comprises additive manufacturing using a 3D printer to create a resin pattern that is then invested and cast [8–10]; the other is selective laser sintering (SLS) [11–13]. Frameworks fabricated by casting 3D-printed resin patterns reportedly show good fit on trial fitting to a working cast; however, slight adjustments by a clinical supervisor are required on fitting to the patient [8]. Conversely, a prosthodontist evaluation of frameworks fabricated by SLS reported good fit on the patient [11]. Compared to frameworks fabricated by conventional casting

* Corresponding author at: Department of Removable Partial Prosthodontics, Tokyo Dental College, 2-9-18 Kandamisakicho Chiyoda-ku, Tokyo, 101-0061, Japan.
E-mail address: atasaka@tdc.ac.jp (A. Tasaka).

https://doi.org/10.1016/j.jpor.2019.07.009
1883-1958/

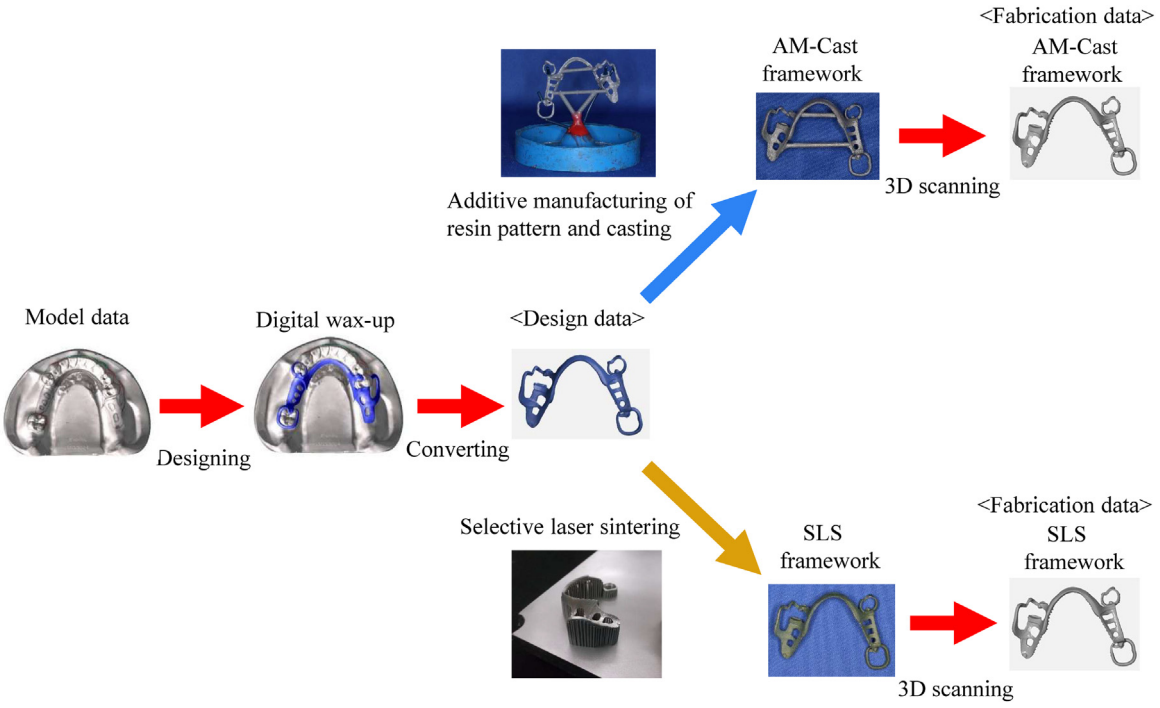

Fig. 1. Flowchart of data capture.
Designing and Converting (Digistell, Digilea).
Additive manufacturing of resin pattern (Projet3510DP; 3D Systems Corporation) and casting (FornaxT; BEGO).
Selective laser sintering (EOSINT M270; EOS).
3D scanning (ATOS Core200; GOM).

methods, those fabricated by SLS show superior fatigue resistance, mechanical properties, and patient satisfaction [14,15].

Various studies have evaluated the fit of frameworks fabricated using CAD/CAM technology [10,13,16,17]. However, it is difficult to accurately interpret fabrication accuracy based on these studies due to limitations such as restriction of fit evaluation to only the rest of the RPD components [16] and intraoral scanner error in the framework fabrication process [17].

The present study hypothesized that different accuracies would be observed for frameworks fabricated by 3D-printed pattern casting compared to those fabricated by SLS depending on the RPD component. Testing this hypothesis should enable clarification of the issues for frameworks fabricated using each technique and the key points for adjusting them. The present study aimed to compare the accuracy of RPD metal frameworks fabricated by 3D-printed pattern casting and those fabricated by SLS.

2. Material and methods

2.1. Fabrication of experimental metal framework

Fig. 1 shows the experimental framework fabrication procedure. A partially edentulous mandibular plaster jaw model (MIS3004-L-PL-28; Nissin Dental Products Inc., Kyoto, Japan) was used for the simulation model. In the model, rest seats were prepared on the distal side of the left mandibular first premolar (tooth #34 [FDI Two-Digit Notation]) and the mesial sides of the left mandibular second molar (tooth #37) and right mandibular second premolar (tooth #45). Guide planes were prepared on the distal proximal surfaces of teeth #34 and #45 and the mesial proximal surface of tooth #37. After 3D-scanning the model using a dental scanner (Smart Big; Open Technologies, Brescia, Italy), CAD software (Digistell; Digilea, Montpellier, France) was used to design the framework (design data). Retainers comprised an Akers clasp at tooth #34, ring clasp at tooth #37, and RPI clasp at tooth #45 with a lingual bar selected as the major connector. To ensure complete filling during casting, accessory sprues were placed between the tips of the buccal and lingual arms of the Akers clasp, the tip of the ring clasp and the rest of tooth #37, and the tip of the RPI clasp and the rest of tooth #45.

For 3D-printed pattern casting of the framework, a resin pattern was formed by additive manufacturing using a 3D printer (ProJet 3510DP; 3D Systems Corporation, Circle Rock Hill, SC, USA). In order to prevent pattern distortion due to resin shrinkage prior to additive manufacturing, two reinforcement bars were added to the design data corresponding to the regions of the framework between teeth #34 and #44, and between teeth #36 and #46, respectively. After printing, the pattern was rapidly invested and cobalt–chromium alloy (Dan Cobalt Chuukou-shitsu; NIHON SHIKA KINZOKU Co., Ltd., Osaka, Japan) was used to cast the framework (AM-Cast framework). For the framework of SLS (SLS framework), a direct metal laser sintering machine (EOSINT M270; EOS, Krailling, Germany) was used. Sintering was performed so that the surfaces important for good framework fit were oriented upward by taking care to ensure parallelism between the occlusal surfaces of the three rests and the sintering machine base plate. A sintering speed of 1100–1200 mm/s, laser spot diameter of 0.08–0.1 mm, and layer thickness of 0.02 mm were used for the SLS framework. Five AM-Cast and five SLS frameworks were fabricated. After casting, the AM-Cast frameworks were sandblasted with 50 μm Al_2O_3 particles at a pressure of 0.5 MPa. After sintering, the SLS frameworks were annealed at 1000 °C for 30 min. Shot peening was subsequently performed with ceramic particles at a pressure of 3.0 bars. After extracting the SLS framework from the base plate and removing the support material, homogenization treatment was performed at 1150 °C for 30 min. Neither framework type was polished.

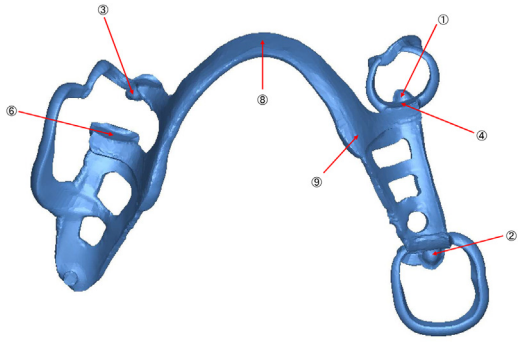

Fig. 2. Measurement site 1.
① Rest: #34.
② Rest: #37.
③ Rest: #45.
④ Proximal plate: #34.
⑥ Proximal plate: #45.
⑧ Lingual bar: center.
⑨ Lingual bar: joining area on the tooth supported side.

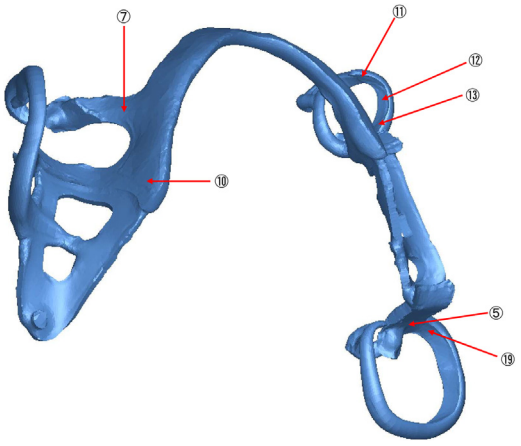

Fig. 3. Measurement site 2.
⑤ Proximal plate: #37.
⑦ Minor connector.
⑩ Lingual bar: joining area on the tooth-tissue supported side.
⑪ Akers clasp: tip of the buccal arm.
⑫ Akers clasp: center of the buccal arm.
⑬ Akers clasp: shoulder of the buccal arm.
⑲ Ring clasp: shoulder.

2.2. Verification of accuracy

The fabricated frameworks were coated with titanium oxide and then scanned with an ATOS Core 80 3D scanner (GOM, Braunschweig, Germany) to obtain 3D data (fabrication data). Accuracy was verified by superimposing the AM-Cast and SLS framework fabrication data on the design data using best fit algorithm of 3D data inspection software (GOM Inspect, GOM) in order to compare shape differences.

A total of 22 measurement sites were compared: three rests (teeth #34, #37, and #45) and three proximal plates at the same sites; one minor connector; three sites on the lingual bar (center and the joining areas on the tooth-supported and tooth-tissue supported sides); six sites on the Akers clasp (tip, center, and shoulder of the buccal and lingual arms); three sites on the ring clasp (tip, center, and shoulder); and three sites on the RPI clasp (tip, center, and base) (Figs. 2–4). At each measurement site, the discrepancy between the design and fabrication data was

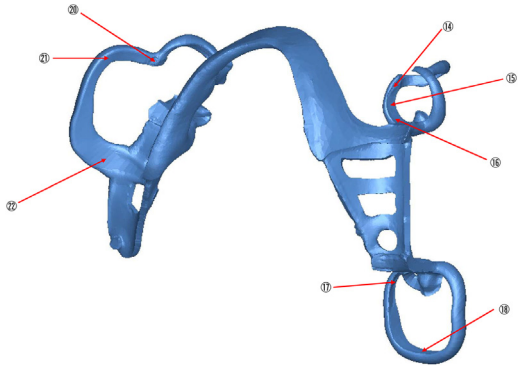

Fig. 4. Measurement site 3.
⑭ Akers clasp: tip of the lingual arm.
⑮ Akers clasp: center of the lingual arm.
⑯ Akers clasp: shoulder of the lingual arm.
⑰ Ring clasp: tip.
⑱ Ring clasp: center.
⑳ RPI clasp: tip.
㉑ RPI clasp: center.
㉒ RPI clasp: bottom.

measured at five points chosen at random on the inner surface of the framework.

Fabrication accuracy was verified using the Mann–Whitney U test to statistically compare the discrepancy between the AM-Cast and SLS frameworks. Significance was set at $p < 0.05$.

3. Results

Figs. 5–7 provide representative examples of color maps showing the shape differences revealed by superimposing the fabrication data onto the design data. Color map of difference value of framework; Yellow to red indicates that the fabrication data was displaced toward the tissue surface relative to the design data (medial displacement). Light blue to blue indicates that the fabrication data was displaced toward the polished surface relative to the design data (lateral displacement). Green indicates minimal displacement. Tables 1–7 show the amount of discrepancy measured at the rests, proximal plates, connectors, and clasp arms.

At the rests, lateral displacement was observed only at tooth #37 for the SLS framework and tooth #45 for the AM-Cast framework. At all other rests, displacement occurred in the opposite direction. At all rests, statistically significant differences in discrepancy were observed between the AM-Cast and SLS frameworks (Table 1).

At the proximal plates, discrepancies were smaller at teeth #34 and #45 for the SLS framework when compared to the AM-Cast framework. However, no statistically significant differences in discrepancy were observed between the AM-Cast and SLS frameworks at tooth #37, where the amounts of discrepancy were almost identical (Table 2).

At the minor connector, lateral displacement was observed for both types of framework; however, a smaller discrepancy was observed for the SLS framework when compared to the AM-Cast framework, and there was a statistically significant difference between the AM-Cast and SLS frameworks.

Regarding the lingual bar, lateral displacement was observed at all sites. At the center, a larger discrepancy was observed for the SLS framework when compared to the AM-Cast framework, and a there was a statistically significant difference between the AM-Cast and SLS frameworks. Conversely, at the joining area on the tooth-supported side of the lingual bar, a larger discrepancy was observed for the AM-Cast framework when compared to the SLS

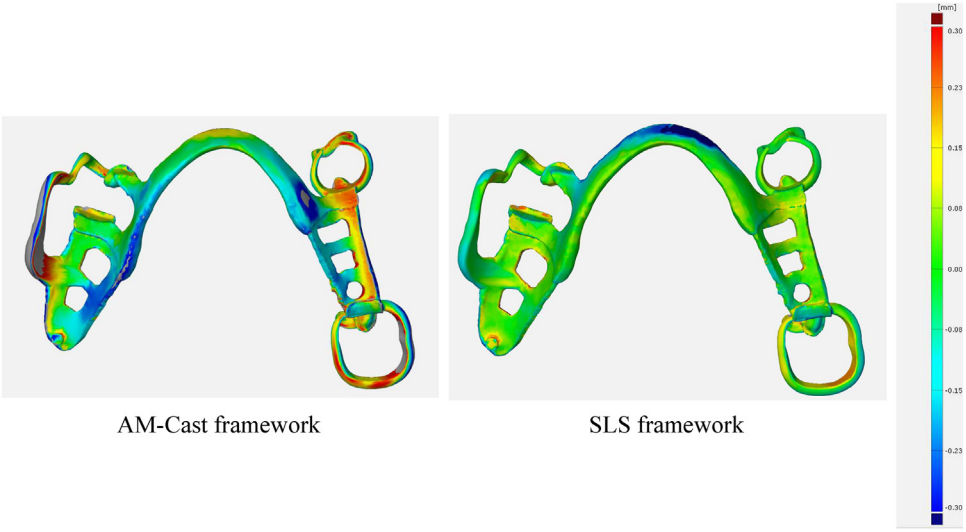

Fig. 5. Color map of shape differences -view from above.

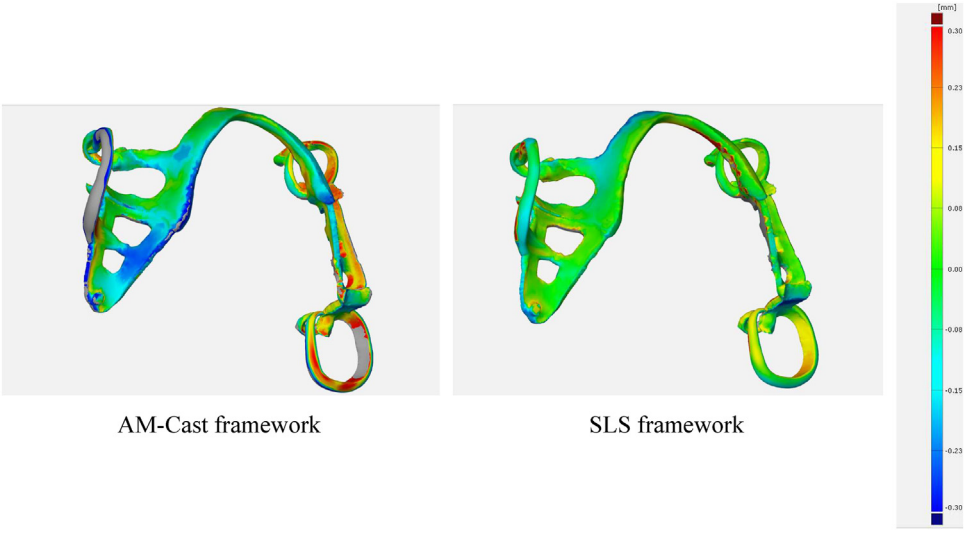

Fig. 6. Color map of shape differences -view from left.

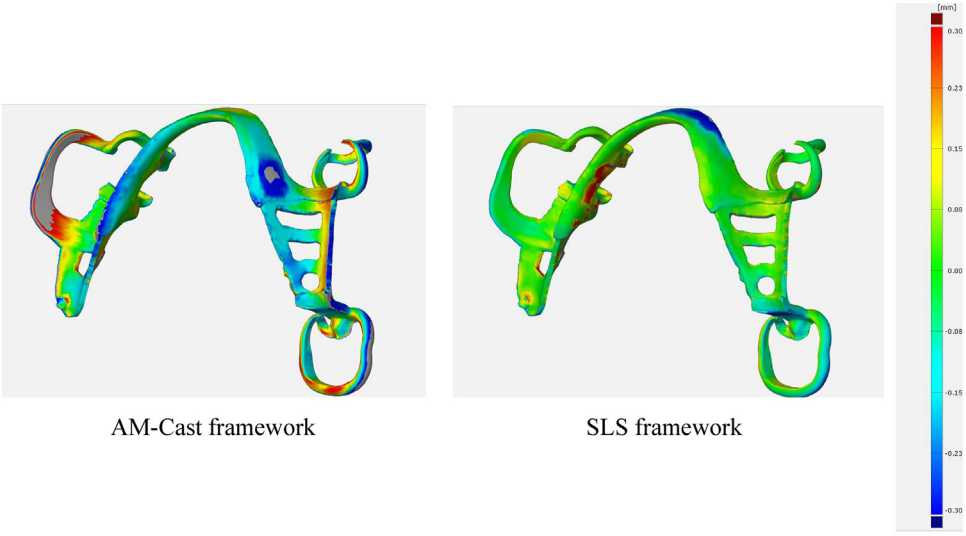

Fig. 7. Color map of shape differences -view from right.

Table 1. Mean, standard deviation, median and interquartile range values of occlusal rest (mm).

Rest		AM-Cast	SLS	P-Value
① #34	Mean	0.125	0.035	
	±SD	0.022	0.010	
	Median	0.114	0.036	0.009
	IQR	0.014	0.010	
② #37	Mean	0.015	−0.126	
	±SD	0.021	0.010	
	Median	0.028	−0.022	0.016
	IQR	0.028	0.012	
③ #45	Mean	−0.032	0.030	
	±SD	0.056	0.005	
	Median	−0.020	0.028	0.015
	IQR	0.038	0.008	

SD = Standard deviation; IQR = Interquartile range.

Table 2. Mean, standard deviation, median and interquartile range values of proximal plate (mm).

Proximal plate		AM-Cast	SLS	P-Value
④ #34	Mean	0.150	0.042	
	±SD	0.028	0.006	
	Median	0.138	0.042	0.009
	IQR	0.040	0.004	
⑤ #37	Mean	−0.132	−0.135	
	±SD	0.073	0.006	
	Median	−0.104	−0.136	0.601
	IQR	0.106	0.008	
⑥ #45	Mean	0.058	−0.018	
	±SD	0.031	0.014	
	Median	0.062	−0.020	0.009
	IQR	0.044	0.020	

SD = Standard deviation; IQR = Interquartile range.

Table 3. Mean, standard deviation, median and interquartile range values of connector (mm).

Connector		AM-Cast	SLS	P-Value
⑦ Minor connector	Mean	−0.103	−0.074	
	±SD	0.014	0.008	
	Median	−0.102	−0.080	0.008
	IQR	0.016	0.010	
⑧ Lingual bar Center	Mean	−0.056	−0.166	
	±SD	0.036	0.009	
	Median	−0.068	−0.170	0.009
	IQR	0.030	0.008	
⑨ Joining area Tooth supported	Mean	−0.185	−0.000	
	±SD	0.138	0.009	
	Median	−0.144	−0.002	0.009
	IQR	0.134	0.004	
⑩ Joining area Tooth-tissue supported	Mean	−0.021	−0.020	
	±SD	0.022	0.007	
	Median	−0.024	−0.018	0.834
	IQR	0.022	0.008	

SD = Standard deviation; IQR = Interquartile range.

framework, and there was a statistically significant difference between the AM-Cast and SLS frameworks. At the joining area on the tooth-tissue supported side of the lingual bar, no statistically significant difference in discrepancy was observed between the AM-Cast and SLS frameworks (Table 3).

Regarding the buccal arm of the Akers clasp, lateral displacement was observed only at the tip for the AM-Cast framework. At all other sites, displacement was medial. At the tip of the buccal arm, no significant difference in discrepancy was observed between the AM-Cast and SLS frameworks. At the center and shoulder of the buccal arm, a larger discrepancy was observed for the AM-Cast framework than the SLS framework, and there was a statistically significant difference between the AM-Cast and SLS frameworks (Table 4). Similarly, in the lingual arm of the Akers

Table 4. Mean, standard deviation, median and interquartile range values of buccal arm of Akers clasp (mm).

Arm		AM-Cast	SLS	P-Value
Akers clasp				
Buccal arm				
⑪ Tip	Mean	−0.031	0.035	
	±SD	0.053	0.017	
	Median	−0.046	0.040	0.076
	IQR	0.060	0.008	
⑫ Center	Mean	0.180	0.036	
	±SD	0.031	0.015	
	Median	0.188	0.036	0.009
	IQR	0.020	0.012	
⑬ Shoulder	Mean	0.158	0.040	
	±SD	0.030	0.006	
	Median	0.150	0.040	0.009
	IQR	0.034	0.008	

SD = Standard deviation; IQR = Interquartile range.

Table 5. Mean, standard deviation, median and interquartile range values of lingual arm of Akers clasp (mm).

Arm		AM-Cast	SLS	P-Value
Akers clasp				
Lingual arm				
⑭ Tip	Mean	−0.126	0.016	
	±SD	0.058	0.022	
	Median	−0.090	0.022	0.009
	IQR	0.072	0.004	
⑮ Center	Mean	0.012	0.042	
	±SD	0.023	0.011	
	Median	0.008	0.048	0.093
	IQR	0.016	0.018	
⑯ Shoulder	Mean	0.108	0.056	
	±SD	0.028	0.008	
	Median	0.114	0.056	0.009
	IQR	0.032	0.008	

SD = Standard deviation; IQR = Interquartile range.

Table 6. Mean, standard deviation, median and interquartile range values of Ring clasp (mm).

Arm		AM-Cast	SLS	P-Value
Ring clasp				
⑰ Tip	Mean	−0.138	−0.035	
	±SD	0.096	0.020	
	Median	−0.094	−0.03	0.028
	IQR	0.106	0.012	
⑱ Center	Mean	0.215	0.123	
	±SD	0.088	0.009	
	Median	0.196	0.124	0.074
	IQR	0.106	0.002	
⑲ Shoulder	Mean	0.117	0.020	
	±SD	0.027	0.002	
	Median	0.108	0.020	0.009
	IQR	0.010	0.000	

SD = Standard deviation; IQR = Interquartile range.

clasp, lateral displacement was observed only at the tip for the AM-Cast framework. At the tip and shoulder of the lingual arm, a larger discrepancy was observed for the AM-Cast framework than the SLS framework, and there was a statistically significant difference between the AM-Cast and SLS frameworks. At the center of the lingual arm, no significant difference in discrepancy was observed between the AM-Cast and SLS frameworks (Table 5). In the ring clasp arm, lateral displacement was observed at the tip for both the AM-Cast and SLS frameworks. The discrepancy tended to be larger at the center for both the AM-Cast and SLS frameworks. Furthermore, at the tip and shoulder, a larger discrepancy was

Table 7. Mean, standard deviation, median and interquartile range values of RPI clasp (mm).

Arm RPI clasp		AM-Cast	SLS	P-Value
⑳ Tip	Mean	0.031	0.030	
	±SD	0.061	0.015	
	Median	0.042	0.036	0.675
	IQR	0.100	0.014	
㉑ Center	Mean	0.352	0.110	
	±SD	0.143	0.012	
	Median	0.370	0.108	0.009
	IQR	0.174	0.014	
㉒ Base	Mean	0.144	−0.029	
	±SD	0.069	0.010	
	Median	0.140	−0.032	0.009
	IQR	0.090	0.006	

SD = Standard deviation; IQR = Interquartile range.

observed for the AM-Cast framework than the SLS framework, and there was a statistically significant difference between the AM-Cast and SLS frameworks (Table 6). Regarding the I bar of the RPI clasp, lateral displacement was observed only at the base for the SLS framework; at all other sites, displacement was medial. Furthermore, at the center and base, a larger discrepancy was observed for the AM-Cast framework than the SLS framework, and there was a statistically significant difference between the AM-Cast and SLS frameworks (Table 7).

4. Discussion

Previous research evaluated the fabrication accuracy of RPD frameworks by measuring the amount of displacement from the working cast [18–20] or space [10,13,21–23] arising at several reference points due to framework distortion. In the majority of studies, framework displacement was only measured in the major connector with no evaluation conducted of the rests, which are particularly important for fit. The amount of space was evaluated by measuring the thickness of the silicone impression material. However, with this technique, distortion and tearing occur when the impression material is removed. Furthermore, it is difficult to specify measurement sites, while the detection limit regarding the thickness of the silicone impression material is around 0.03 mm [21]. Although the amount of space between clasps and abutment teeth can be measured using 0.5 mm orthodontic wire, this method lacks objectivity [23]. In the present study, software superimposition of framework fabrication and design data enabled quantitative, comprehensive evaluation of accuracy. Presenting the data as color maps also enabled 3D evaluation of the direction of displacement. The margins of error of the software used in the present study were 0.012 mm for inter-point measurements and 0.015 mm for surface measurements.

The present study used Material Jetting to print the casting pattern. This method enables printing with a smooth surface at an accuracy of 29–32 μm. However, as the material used is cured by ultraviolet light, distortion due to sunlight-related degradation is possible [24]. To avoid this effect, the present casting pattern was rapidly invested after printing. Casting shrinkage of metal alloys can occur due to solidification shrinkage and thermal contraction from the solidification temperature down to room temperature. The present study used a cobalt–chromium alloy, which has a casting shrinkage of 2.3% [25].

Stern et al. reported the mean space between the rest and the corresponding rest seat in metallic dentures fabricated by conventional casting as 173–215 μm [21]. Meanwhile, Dunham et al. reported the same value as 193 ± 203 μm (range, 0–828 μm) [22]. The discrepancies (absolute displacement values) at the rests in the frameworks fabricated in the present study were within this range in both the AM-Cast and SLS framework conditions. However, as both lateral and medial displacement of the rests in the frameworks fabricated in the present study was observed in relation to the design data depending on the measurement site, each site should be carefully inspected at the time of trial fitting of the framework to the model for anything that might prevent complete alignment between the rest and rest seat.

Lee et al. reported displacement of 70.37–152.5 μm at the proximal plates in a framework fabricated by casting using a 3D-printed resin pattern [10]. Similar values were obtained in the present study at the proximal plates for the AM-Cast framework. Accuracy tended to be better at the proximal plates for the SLS framework compared to the AM-Cast framework; however, the amount of discrepancy differed greatly depending on the site. The present findings suggest that accuracy may be affected by whether the structure of the proximal plate is independent from (tooth #45) or joined to (teeth #34 and #37) the clasp arm and rest.

Regarding the connectors, large lateral discrepancies were observed at the joining area on the tooth-supported side of the lingual bar for the AM-Cast framework. This site matched the site of the joint between the cast pattern and the reinforcement bar. With the reinforcement bar functioning as a sprue, localized casting shrinkage may have occurred at the joint [26]. Therefore, when a reinforcement bar is placed in the cast pattern, either it should be added to the retention grid, which does not affect the fit of the framework, or a reservoir should be added to the reinforcement bar. Conversely, large, localized discrepancies were observed at the center of the lingual bar for the SLS framework, likely due to buckling distortion produced during SLS [27]. As this kind of residual stress affects not only fit but also strength [28], further investigation is required regarding sintering conditions. Recent attention has focused on simulations to predict distortion and residual stress during SLS using computer-aided engineering (CAE) [29]. As CAE can deliver product optimization as well as reduced fabrication time and costs, further software development and adoption are awaited.

In the clasp arm, lateral displacement was observed at the tips of the Akers and ring clasps for the AM-Cast framework. Similar results were obtained in a study of Akers clasps alone without framework fabricated by 3D-printed pattern casting [30]. Conversely, medial displacement was observed at the tip of the RPI clasp as an infrabulge clasp for the AM-Cast framework, the opposite displacement direction to suprabulge clasps. Firtell et al. reported different accuracies at the tips of suprabulge and infrabulge clasps, with the tips of suprabulge clasps placed in less and those of infrabulge in more undercut than prescribed [31]. The present findings suggest that the effects of casting pattern distortion and shrinkage on tip displacement differ depending on the form of clasp arm. Although overall accuracy tended to be better for the clasp arm of the SLS framework compared to that of the AM-Cast framework, large discrepancies were observed at the center of the ring and RPI clasp arms. As the long, thin clasps may be susceptible to the same distortion as the lingual bar, caution should be exercised when using SLS.

SLS machines are large and require significant capital investment. Conversely, 3D printers, which can create items such as casting patterns, dental models, custom trays, and splints from resin with additive manufacturing, are small and relatively affordable. Frameworks can also be fabricated using computer numerical controlled milling techniques; however, considerable metal is wasted, and cutting tools are damaged during milling, and consequently cause poor cost performance. Therefore, computer numerical controlled milling techniques are not used in clinical settings. Each specific CAD/CAM technology should be selected based on careful consideration of the economic, productivity-related, environmental, and other advantages and disadvantages

[32]. Under the present experimental conditions, overall discrepancies and interquartile range were smaller for the SLS framework compared to the AM-Cast framework, suggesting superior fabrication accuracy and reproducibility with SLS.

The present study had the following limitations. Due to the difficulty of obtaining design data completely identical to the shape of a conventional wax-up, frameworks made by conventional casting could not be included as one of the experimental conditions. Other experimental techniques and analyzers need to be developed to compare frameworks fabricated using CAD/CAM technology with conventional methods. Furthermore, only one design pattern was used to represent a typical partially edentulous mandible. Various designs are possible depending on the site and extent of the edentulous region. In particular, the configuration of the major connector, for which accuracy was an issue in the SLS framework, is very different in the maxilla. The degree of variation underlies a need for further investigation.

5. Conclusions

Between AM-Cast and SLS, the fabrication accuracies of RPD metal frameworks differed depending on the specific structural component. However, overall discrepancies were smaller for the SLS framework compared to the AM-Cast framework, suggesting superior fabrication accuracy and reproducibility with SLS.

Conflicts of interest

There are no conflicts of interest with regard to this study.

References

[1] Arafa KAO. Assessment of the fit of removable partial denture fabricated by computer-aided designing/computer aided manufacturing technology. Saudi Med J 2018;39:17–22.
[2] Williams RJ, Bibb R, Rafik T. A technique for fabricating patterns for removable partial denture frameworks using digitized casts and electronic surveying. J Prosthet Dent 2004;91:85–8.
[3] Eggbeer D, Bibb R, Williams R. The computer-aided design and rapid prototyping fabrication of removable partial denture frameworks. Proc Inst Mech Eng H 2005;219:195–202.
[4] Wang Y, Zhao YJ, Wu L, Lu PJ. Preliminary study on CAD of removable partial denture framework. Appl Mech Mater 2012;220-3:2777–82.
[5] Hussein MO, Hussein LA. Novel 3D modeling technique of removable partial denture framework manufactured by 3D printing technology. Int J Adv Res 2014;9:686–94.
[6] Lima JM, Anami LC, Araujo RM, Pavanelli CA. Removable partial dentures: use of rapid prototyping. J Prosthodont 2014;23:588–91.
[7] Alifui-Segbaya F, Williams RJ, George R. Additive manufacturing: a novel method for fabricating cobalt–chromium removable partial denture frameworks. Eur J Prosthodont Restor Dent 2017;25:73–8.
[8] Bibb RJ, Eggbeer D, Williams RJ, Woodward A. Trial fitting of a removable partial denture framework made using computer aided design and rapid prototyping techniques. Proc Inst Mech Eng H 2006;220:793–7.
[9] Wu J, Wang X, Zhao X, Zhang C, Gao B. A study on the fabrication method of removable partial denture framework by computer-aided design and rapid prototyping. Rapid Prototyping J 2012;18:318–23.
[10] Lee JW, Park JM, Park EJ, Heo SJ, Koak JY, Kim SK. Accuracy of a digital removable partial denture fabricated by casting a rapid prototyped pattern: a clinical study. J Prosthet Dent 2017;118:468–74.
[11] Bibb R, Eggbeer D, Williams R. Rapid manufacture of removable partial denture frameworks. Rapid Prototyping J 2006;12:95–9.
[12] Williams RJ, Bibb R, Eggbeer D, Collis J. Use of CAD/CAM technology to fabricate a removable partial denture framework. J Prosthet Dent 2006;96:96–9.
[13] Ye H, Ning J, Li M, Niu L, Yang J, Sun Y, et al. Preliminary clinical application of removable partial denture frameworks fabricated using computer-aided design and rapid prototyping techniques. Int J Prosthodont 2017;30:348–53.
[14] Alageel O, Abdallah MN, Alsheghri A, Song J, Caron E, Tamimi F. Removable partial denture alloys processed by laser-sintering technique. J Biomed Mater Res B Appl Biomater 2018;106:1174–85.
[15] Almufleh B, Emami E, Alageel O, de Melo F, Seng F, Caron E, et al. Patient satisfaction with laser-sintered removable partial dentures: a crossover pilot clinical trial. J Prosthet Dent 2018;119:560–7.
[16] Arnold C, Hey J, Schweyen R, Setz JM. Accuracy of CAD-CAM-fabricated removable partial dentures. J Prosthet Dent 2018;119:586–92.
[17] Soltanzadeh P, Suprono MS, Kattadiyil MT, Goodacre C, Gregorius W. An in vitro investigation of accuracy and fit of conventional and CAD/CAM removable partial denture frameworks. J Prosthodont 2019;28:547–55, doi: http://dx.doi.org/10.1111/jopr.12997.
[18] Diwan R, Talic Y, Omar N, Sadiq W. The effect of storage time of removable partial denture wax pattern on the accuracy of fit of the cast framework. J Prosthet Dent 1997;77:375–81.
[19] Gowri V, Patil NP, Nadiger RK, Guttal SS. Effect of anchorage on the accuracy of fit in removable partial denture framework. J Prosthodont 2010;19:387–90.
[20] Ali M, Nairn RI, Sherriff M, Waters NE. The distortion of cast cobalt—chromium alloy partial denture frameworks fitted to a working cast. J Prosthet Dent 1997;78:419–24.
[21] Stern MA, Brudvik JS, Frank RP. Clinical evaluation of removable partial denture rest seat adaptation. J Prosthet Dent 1985;53:658–62.
[22] Dunham D, Brudvik JS, Morris WJ, Plummer KD, Cameron SM. A clinical investigation of the fit of removable partial dental prosthesis clasp assemblies. J Prosthet Dent 2006;95:323–6.
[23] Keltjens HM, Mulder J, Käyser AF, Creugers NH. Fit of direct retainers in removable partial dentures after 8 years of use. J Oral Rehabil 1997;24:138–42.
[24] Revilla-León M, Özcan M. Additive manufacturing technologies used for processing polymers: current status and potential application in prosthetic dentistry. J Prosthodont 2019;28:146–58, doi:http://dx.doi.org/10.1111/jopr.12801.
[25] Pulskamp FE. A comparison of the casting accuracy of base metal and gold alloys. J Prosthet Dent 1979;41:272–6.
[26] Burnett CA, Maguire H. Sprue design in removable partial denture casting. J Dent 1996;24:99–103.
[27] Malekjafarian A, OBrien EJ, Micu LA. Investigation of buckling capacity of metal materials manufactured by laser 3D printing. Procedia Manuf 2017;7:696–700.
[28] Kruth JP, Mercelis P. Residual stresses in selective laser sintering and selective laser melting. Rapid Prototyp J 2006;5:254–65.
[29] Li C, Fu CH, Guo YB, Fang FZ. Fast prediction and validation of part distortion in selective laser melting. Procedia Manuf 2015;1:355–65.
[30] Tasaka A, Kato Y, Odaka K, Matsunaga S, Goto Tazuko K, Abe Shinich, et al. Accuracy of clasp fabricated by casting, milling and selective laser melting using CAD/CAM technology. Int J Prosthodont 2019 in press.
[31] Firtell DN, Muncheryan AM, Green AJ. Laboratory accuracy in casting removable partial denture frameworks. J Prosthet Dent 1985;54:856–62.
[32] Koutsoukis T, Zinelis S, Eliades G, Al-Wazzan K, Rifaiy MA, Al Jabbari YS. Selective laser melting technique of Co–Cr dental alloys: a review of structure and properties and comparative analysis with other available techniques. J Prosthodont 2015;24:303–12.